

Analysis of the Change of Tidal Flat Area in Jiangsu in the Past 20 Years Using Hydrodynamic Model and Landsat Data

Kaizheng Wang¹, HuanLi¹, Zeyu Han¹, Jin Wang¹ and Weibo Lin²

¹College of Harbour, Coastal and Offshore Engineering, Hohai University, Nanjing, China

²Tidal Flat Research Center of Jiangsu Province, Nanjing, China

Keywords: Landsat, Delft3D, Coastline Change, Tidal Flat Area.

Abstract: Based on the Landsat series data, this paper interprets the remote sensing images of the coastal areas of Jiangsu in 2001, 2011, and 2021, cooperates with the hydrodynamic model and the measured slope, calculates the average spring tide line, and defines the area between the coastline and the average spring low tide line as a tidal flat. Area, and analyze the changes in the Jiangsu coastline and tidal flat area in the past 20 years. The results show that from 2001 to 2021, the coastline of Jiangsu has increased by nearly 17%, with an average annual growth rate of 6 km/a, and the tidal flat area has decreased by nearly 10%, with an average annual decrease rate of 17.31 km²/a.

1 INTRODUCTION

In recent years, with the rapid development of the global economy, coastal cities have made unprecedented efforts to develop and utilize coastal areas. Especially in the context of global climate change and rising sea levels, coastlines have undergone drastic changes. More than half of the world's coastlines have been eroded and retreated (Dar & Dar, 2009). It has an enormous impact on ecology, the environment, and the economy of society. For the coast of China, due to tidal tides, storm surges, and super-intensive reclamation, the position of the coastline is constantly changing, and the tidal flat area is reduced (Murray, 2014; Wu, Hou, & Xu, 2014; Y. et al., 2022). Therefore, the monitoring and protection of coastal zones are becoming more and more important, which has important practical significance for ecological protection and national development.

There are generally two methods for obtaining information on coastal areas: field measurement and remote sensing technology monitoring. The traditional field survey is to use various instruments and means to directly obtain tidal flat information through the field survey (Allen & Duffy, 1998; Lawler, 2006; R. et al., 2002). Remote sensing

technology can obtain information quickly and in a large area, and it has an advantage that cannot be underestimated for the difficulty of obtaining information in the complex and changeable coastal zone (Liu, Li, Zhou, Yang, & Mao, 2013; Lohani, 1999; Mason, Davenport, Robinson, Flather, & McCartney, 1995; Ryu et al., 2008; Samuel, Huan, Ebenezer, Temitope, & Zheng, 2022; Weiqi et al., 2021; Xuhui et al., 2021). Previous studies on tidal flat area changes only used low-tide images to extract tidal flat areas. Due to differences in tidal levels, there is no unified benchmark for tidal flat extraction, and it is difficult to compare.

This paper intends to use a combination of field measurement, remote sensing technology, numerical simulation, and GIS technology to visually interpret the remote sensing images of the coastal areas of Jiangsu in 2001, 2011, and 2021, and extract the Jiangsu coastline and instantaneous water edge in each time phase. By establishing the Jiangsu coastal hydrodynamic model to obtain the instantaneous tidal level value of the waterside line, and synergistically with the slope prediction analysis method, the average spring tide low tide line is calculated. The area between the coastline and the average spring and low tide line is defined as the tidal flat area, and we

analyze the changes in the Jiangsu coastline and tidal flat area in the past 20 years.

2 MATERIALS AND METHODS

2.1 Study Area

This paper selects the coastal flat of Jiangsu as the study area. The coast of Jiangsu starts from the mouth

of Xiuzhen River in the north and reaches Lianxing Port in the east of Qidong in the south. For the convenience of statistics, according to the characteristics of the coastline of Jiangsu Province, the coastline of Jiangsu Province is divided into three sections: the northern section (Xiaozhen River Estuary - Biandan River Estuary), the middle section (Biandan River Estuary - Tuanjie Port), and the southern section (Tuanjie Port - Lianxing Port).

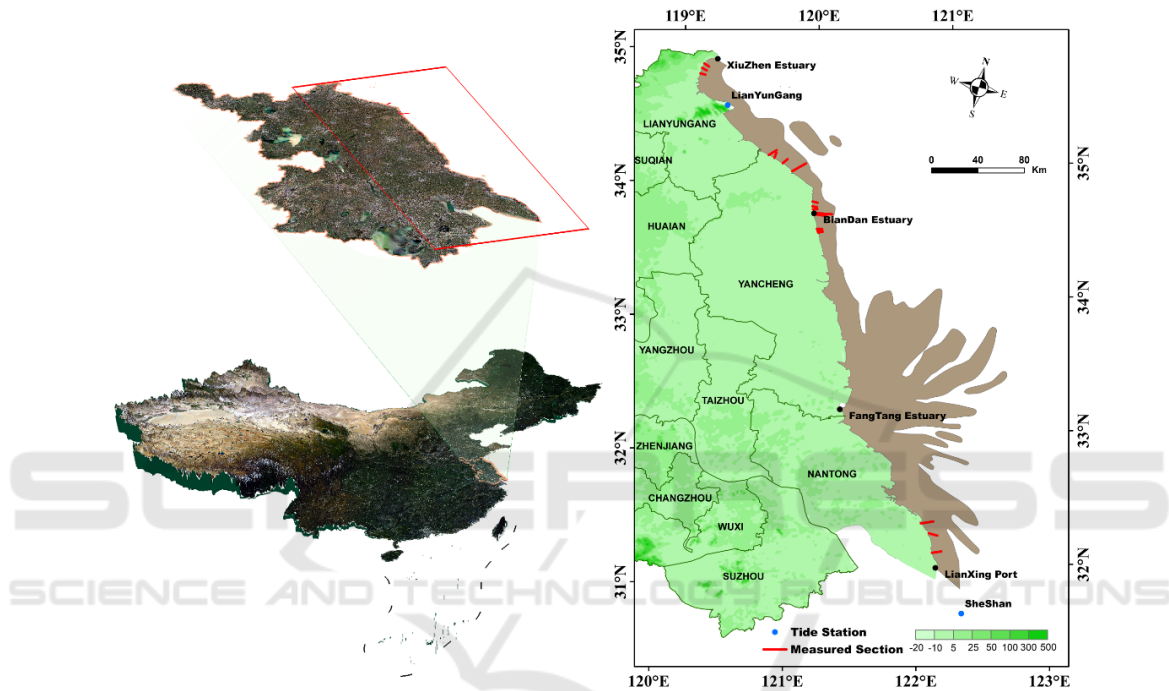


Figure 1: Location of the study area.

2.2 Data Acquisition and Processing

The remote sensing data selected Landsat-7 ETM+ and Landsat-8 OLI images with low cloud content and high definition in 2001, 2011, and 2021, a total of 9 images, and performed geometric correction and image enhancement preprocessing on the remote sensing images. The measured section data adopts the topographic data of 22 sections along the coast of Jiangsu Province obtained in April and September 2021 (Figure 1).

Table 1: Remote sensing image information

Region	Sensor	Year
North	Landsat 7 ETM+	2001、2011
North	Landsat 8 OLI	2021
Middle	Landsat 8 OLI	2021
Middle	Landsat 7 ETM+	2001、2011
South	Landsat 7 ETM+	2001、2011
South	Landsat 8 OLI	2021

2.3 Methods

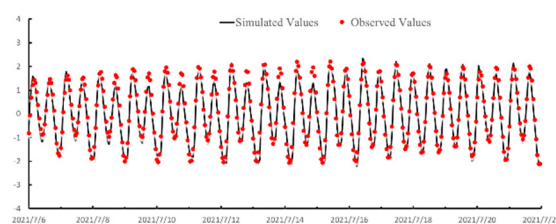
2.3.1 Shoreline Extraction

The artificial coastline is subject to seawall, and the natural coastline is discussed in the following situations.

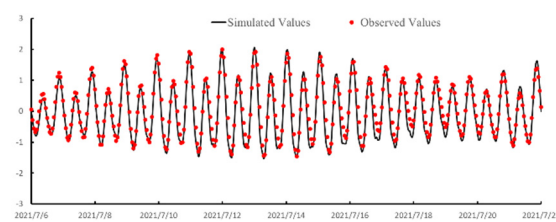
Bedrock shoreline: A bedrock shoreline refers to a coastline composed of exposed bedrock. The location of the bedrock shoreline is defined as the trace line of the sea-land boundary or the base of the cliff at the average spring tide level for many years; **Sandy shoreline:** Sandy shoreline refers to the shoreline composed of sandy and gravelly sandstone. The sandy shoreline is generally relatively straight, and the upper part of the beach is often piled up into ridged sandy sediment parallel to the shore, called a beach ridge. The coastline is generally defined on the seaward side of the top of the beach ridge; **Muddy shoreline:** the muddy coast is mainly a low and flat coast shaped by tidal action, and the intertidal width is wide and gentle. The coastline should be defined according to the comprehensive analysis of the trace line of the sea-land boundary at the average high tide level of the spring tide for many years, as well as the trace line of the distribution of coastal vegetation, plant debris, shell fragments, etc. **Estuary shoreline:** The tidal gate (dam) outer boundary line or the first bridge is used as the estuary shoreline. If the tidal sluice (dam) or the first bridge is too deep inland, the prominent point where the estuary suddenly widens is selected as the estuary shoreline.

2.3.2 Hydrodynamic Model Establishment

To obtain the tidal level values of discrete points in a typical area, a hydrodynamic model is established. This time, Delft3D software was used for hydrodynamic simulation. The tidal level data of Lianyungang and Sheshan stations were collected for model verification, and the root mean square errors (RMSE) of tidal levels were 0.32m and 0.29m respectively. The distribution of the stations is shown in Figure 1, and the model verification results are shown in Figure 2.



(a) Lianyungang



(b) Sheshan

Figure 2: Tide level verification result.

2.3.3 Average Spring Tide and Low Tide Line Projection

(1) Instantaneous Waterline Discretization

The water's edge is the boundary between the water body and the tidal flat at the time of remote sensing image imaging. The low tide remote sensing image is selected, and the visual interpretation method is used to extract the instantaneous waterline. Due to the large spatial range covered by the image, different locations on the waterline at the same time have different tide levels, so it is necessary to divide the instantaneous waterline for assignment. In this paper, we first use the ArcGIS buffer tool to draw a baseline of 800m from the water's edge to the seaside and then use the DASA tool to draw a vertical line every 500 meters on the baseline as split lines. There is a total of 707 split lines in Jiangsu Province, and the intersection of the waterline and the split lines, discrete points, is extracted through ArcGIS.

(2) Tide Level Assignment and Slope Calculation

Based on the established hydrodynamic model, the tide level is extracted at the time of image imaging, and then the tide level is assigned to the corresponding discrete points.

The slope calculation of discrete points is to calculate the slope by selecting the measured data of 22 sections along the coast of Jiangsu Province. The data includes the measured points' longitude, latitude, and elevation information. The formula is as follows (i : Average slope; L : The distance between two adjacent measuring points; z : Elevation of two adjacent measuring points; x, y : Coordinates of two adjacent measuring points)

$$i = \frac{i_1 + i_2 + \dots + i_{n-1} + i_n}{n} \quad (1)$$

$$i_j = \frac{z_j - z_{j+1}}{L} \quad (j = 1, 2, \dots, n) \quad (2)$$

$$L_j = \sqrt{(x_{j+1} - x_j)^2 + (y_{j+1} - y_j)^2} \quad (3)$$

Through the above formula, the slope of each section is calculated. According to the geographical location, sections 1-8 are classified as the northern area, sections 9-18 are classified as the central area, and sections 19-22 are classified as the southern area. The average value of the slopes of all sections in the region is taken as the slope of the region, and finally, the slopes of the northern, middle and southern regions are 6.20%, 1.42%, and 8.73%, respectively.

(3) Average Spring Tide and Low Tide Line Projection

The average spring tide low tide line is calculated based on the tide level assignment results and the slope calculation results. The calculation formula is as follows:

$$\tan \alpha_1 = \tan \alpha \times \frac{\sqrt{(a_2 - a_1)^2 + (b_2 - b_1)^2}}{a_2 - a_1} \quad (4)$$

$$\tan \alpha_2 = \tan \alpha \times \frac{\sqrt{(a_2 - a_1)^2 + (b_2 - b_1)^2}}{b_2 - b_1} \quad (5)$$

$$x = a_1 + \frac{h_1 - h_0}{\tan \alpha_1} \quad (6)$$

$$y = b_1 + \frac{h_1 - h_0}{\tan \alpha_2} \quad (7)$$

In the formula: α_1 、 α_2 are the projected angles of the slope in the longitude and latitude directions, α is the slope assigned by discrete points, (a_1, b_1) (a_2, b_2) are the longitude and latitude coordinates

of the two points on the dividing line, x, y are the longitude and latitude coordinates of the discrete points on the average spring tide and low tide line, and h_0, h_1 are the tidal heights and the average spring tide and low tide levels at the discrete points.

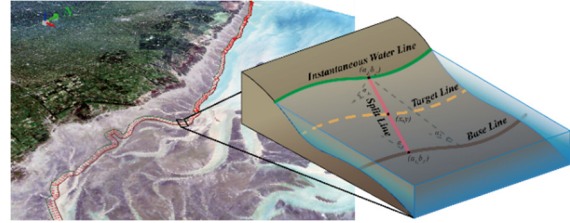


Figure 3: Calculation of discrete points of Multi-year average low tide line

According to the results of the hydrodynamic model, the low tide level of the spring tide is extracted in each discrete point area. According to the above formula, the latitude and longitude coordinates of the discrete points of the average low tide level of the spring tide are calculated, and the calculated discrete points are connected in sequence to form a line, that is, the average low tide line of the spring tide is obtained.

3 RESULTS AND ANALYSIS

3.1 Coastline Change

The coastlines are classified into artificial coastlines, natural coastlines, and estuary coastlines.

The results show that (Table 2), from 2001 to 2021, the coastline of Jiangsu Province as a whole was mainly advancing to the sea, and the length of the coastline increased from 728.69km to 849.67km. Among them, the natural coastline decreased from 526.51km to 301.03km. It has increased from 197.92km to 542.40km, and the estuary line has increased from 4.25km to 6.23km.

Table 2: Coastline length in Jiangsu Province in 2001, 2011, and 2021 (km).

Region	Year	Natural	Artificial	Estuary	All
North	2001	83.79	122.02	2.00	207.81
	2011	82.41	127.62	2.23	212.26
	2021	81.41	176.89	2.33	260.64
Middle	2001	219.69	42.47	1.97	264.13
	2011	204.96	63.27	2.54	270.76
	2021	148.54	167.73	2.62	318.88
South	2001	223.03	33.43	0.29	256.75
	2011	131.57	143.12	0.86	275.55
	2021	71.09	197.78	1.56	270.43
All	2001	526.51	197.92	4.25	728.69
	2011	418.93	334.28	5.37	758.58
	2021	301.03	542.40	6.23	849.67

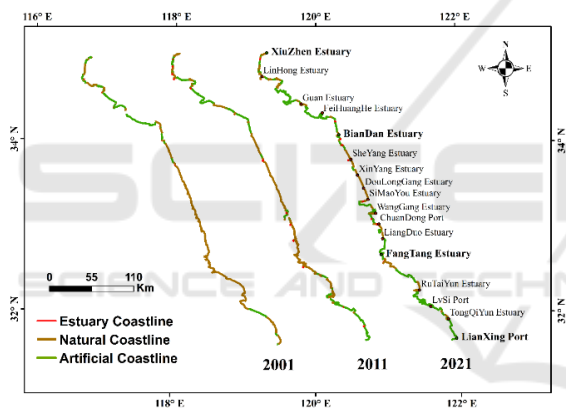


Figure 4: Coastline of Jiangsu Province in 2001, 2011 and 2021.

The northern coastline increased from 207.81km to 260.64km from 2001 to 2021, of which the natural coastline decreased from 83.79km to 81.41km, the artificial coastline increased from 122.02km to 176.89km, and the river port line increased from 2km to 2.33km.

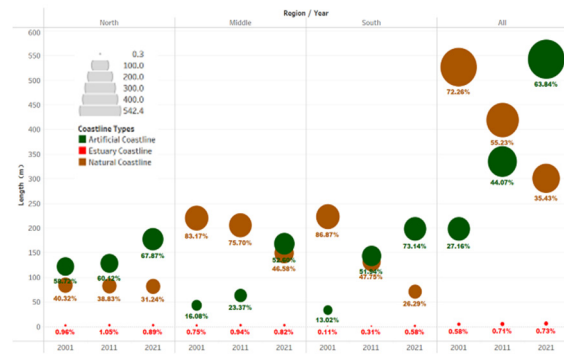


Figure 5: Variation of coastline length in Jiangsu Province.

During 2001-2021, the central coastline increased from 264.13km to 318.88km, of which the natural coastline decreased from 219.69km to 148.54km, the artificial coastline increased from 42.47km to 167.73km, and the river port line increased from 1.97km to 2.62km.

The southern coastline increased from 256.75km to 270.43km during 2001-2021, of which the natural coastline decreased from 223.03km to 71.09km, the artificial coastline increased from 33.43km to 197.78km, and the river port coastline increased from 0.29km to 1.56km.

3.2 Changes in the Area of Tidal Flats

The upper boundary of the tidal flat is the coastline, and the lower boundary is on the calculated average spring and low tide line. The final calculation of the tidal flat area along the Jiangsu coast in 2001 is 3447.22 km², and the tidal flat area along the Jiangsu coast in 2021 is 3100.94 km².

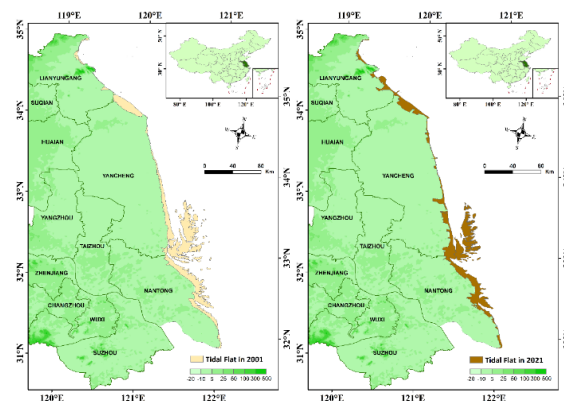


Figure 6: Tidal flats in Jiangsu Province in 2001 and 2021.

The area of tidal flats in Jiangsu Province has decreased by nearly 10% from 2001 to 2021, with an average annual decrease rate of 17.31 km²/a.

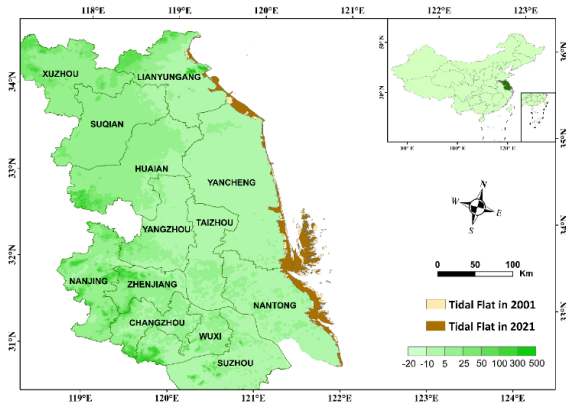


Figure 7: Overlay map of tidal flats in Jiangsu Province in 2001 and 2021.

4 CONCLUSIONS

Based on multi-temporal remote sensing image data and topographic survey data, combined with numerical simulation technology, the evolution characteristics of the coastline in Jiangsu Province and the distribution of monitoring tidal flat resources are analyzed. The main conclusions are as follows:

- (1) From 2001 to 2021, the length of the coastline shows an overall increasing trend, in which the artificial coastline has increased significantly and the natural coastline has decreased.
- (2) From 2001 to 2021, the area of coastal tidal flats in Jiangsu Province has decreased significantly, and active measures should be taken to maintain the stability of tidal flat resources.

ACKNOWLEDGEMENTS

National Natural Science Foundation of China (NSFC, grant no. 41976156)

This work was supported in part by the Marine Science and Technology Innovation Project of Jiangsu Province under Grant JSZRHYKJ202214, in part by the Carbon Peak Carbon Neutral Science and Technology Innovation Projects of Jiangsu Province under Grant BK20220020, and in part by the National

Natural Science Foundation of China under Grant 41401371.

REFERENCES

- Allen, J.R.L., & Duffy, M.J. (1998). Medium-term sedimentation on high intertidal mudflats and salt marshes in the Severn Estuary, SW Britain: the role of wind and tide. *Marine Geology*, 150(1).
- Dar, Imran A., & Dar, Mithas A. (2009). Prediction of Shoreline Recession Using Geospatial Technology: A Case Study of Chennai Coast, Tamil Nadu, India. *Journal of Coastal Research*, 25(6).
- Lawler, D.M. (2006). Advances in the continuous monitoring of erosion and deposition dynamics: Developments and applications of the new PEEP-3T system. *Geomorphology*, 93(1).
- Liu, Yongxue, Li, Manchun, Zhou, Minxi, Yang, Kang, & Mao, Liang. (2013). Quantitative Analysis of the Waterline Method for Topographical Mapping of Tidal Flats: A Case Study in the Dongsha Sandbank, China. *Remote Sensing*, 5(11).
- Lohani, B. (1999). Construction of a Digital Elevation Model of the Holderness Coast using the waterline method and Airborne Thematic Mapper data. *International Journal of Remote Sensing*, 20(3).
- Mason, D. C., Davenport, I. J., Robinson, G. J., Flather, R. A., & McCartney, B. S. (1995). Construction of an inter-tidal digital elevation model by the 'Water-Line' Method. *Geophysical Research Letters*, 22(23).
- Murray, N. J., Clemens, R. S., Phinn, S. R., Possingham, H. P., & Fuller, R. A. (2014). Tracking the rapid loss of tidal wetlands in the Yellow Sea. *Frontiers in Ecology and the Environment*, 12(5).
- R., Cahoon D., C., Lynch J., P., Hensel, R., Boumans, C., Perez B., B., Segura, & W., Day J. (2002). High-Precision Measurements of Wetland Sediment Elevation: I. Recent Improvements to the Sedimentation-Erosion Table. *Journal of Sedimentary Research*, 72(5).
- Ryu, Joo-Hyung, Kim, Chang-Hwan, Lee, Yoon-Kyung, Won, Joong-Sun, Chun, Seung-Soo, & Lee, Saro. (2008). Detecting the intertidal morphologic change using satellite data. *Estuarine, Coastal and Shelf Science*, 78(4).
- Samuel, Daramola, Huan, Li, Ebenezer, Otoo, Temitope, Idowu, & Zheng, Gong. (2022). Coastal evolution

assessment and prediction using remotely sensed front vegetation line along the Nigerian Transgressive Mahin mud coast. *Regional Studies in Marine Science*(prepublish).

- Wei qi, Dai, Huan, Li, Zheng, Gong, Zeng, Zhou, Yuan, Li, Lizhu, Wang, Hongyang, Pei. (2021). Self-organization of salt marsh patches on mudflats: Field evidence using the UAV technique. *Estuarine, Coastal and Shelf Science*, 262.
- Wu, Ting, Hou, Xiyong, & Xu, Xinliang. (2014). Spatio-temporal characteristics of the mainland coastline utilization degree over the last 70 years in China. *Ocean and Coastal Management*, 98.
- Xuhui, Zhang, Huan, Li, Zheng, Gong, Zeng, Zhou, Wei qi, Dai, Lizhu, Wang, & Samuel, Daramola. (2021). Method for UAV-based 3D topography reconstruction of tidal creeks. *Journal of Geographical Sciences*, 31(12).
- Y., Pan, S., Yin, Y.P., Chen, Y.B., Yang, C.Y., Xu, & Z.S., Xu. (2022). An experimental study on the evolution of a submerged berm under the effects of regular waves in low-energy conditions. *Coastal Engineering*, 176.

